# Path following with security margin: A new control algorithm for wheeled Robots

T. Hamel†, P. Souères‡, D. Meizel†
†*UTC/HEUDIASYC.URA CNRS 817, BP 649, 60206 Compiègne, FRANCE*
‡*LAAS-CNRS 7 Av. du Colonel Roche, 31077 Toulouse Cedex 4 FRANCE*
e-mail: thamel@hds.utc.fr, soueres@laas.fr, dmeizel@hds.utc.fr

## Abstract

This paper addresses the problem of determining a feedback control law, robust with respect to localization errors, allowing a mobile robot to follow a prescribed path. The model we consider is a dynamic extension of the usual kinematic model of a car, in the sense that we define the path curvature as a new state variable. The control variables are respectively the linear velocity and the derivative of the curvature. By defining a sliding manifold we determine a stabilizing controller for the nominal system i.e. when the exact configuration is supposed to be known. Then, using Lyapunov analysis, we prove that the system remains stable when the estimated values are used for feedback instead of the exact ones, and we characterize the robustness with respect to localization and curvature estimation errors. The result is expressed by determining a bounded attractive domain where the vehicle's configuration could possibly lie when the closed-loop control is performed with the estimated state values. This domain allows to compute easily a security margin for obstacle avoidance during the path-following phase. Experimental results are presented at the end of the paper.

**Key Words:** Mobile Robots, Robustness, Path-following control, Lyapunov analysis, sliding surfaces.

## 1 Introduction

One difficult question inherently linked to mobile robots' autonomy is the design of feedback control laws allowing to stabilize the motion of wheeled robots. Indeed, on account of the nonholonomic nature of those systems, most part of classical control techniques turn out to be inefficient to solve this problem. The question has motivated a large number of research works for the past ten years. In the literature, this problem called *navigation problem* is commonly divided into three subproblems which are: path following, trajectory tracking, and point stabilization (see [1]).

As the central problem is stated in terms of designing closed-loop controllers taking into account the kinematic nonholonomic rolling without slipping constraint, very few research works have tried to integrate the vehicle's dynamics in their model. The works by [2] and [3]constitute an interesting effort in this direction.

Commonly, the other works devoted to this problem only have considered kinematic models. Nonlinear feedback controllers have been proposed (See [4] and [5]. The main idea, behind these algorithms, is to define velocity control inputs stabilizing the closed-loop system. However neglecting the robot's dynamics induces strong limitation in practice. Considering a kinematic model, it can be very satisfactory, from a theoretical point of view, to use a static controller assuming that the reference path has a continuous curvature. However, most part of the existing path planners propose path along which the curvature is only almost everywhere continuous. See for instance the nonholonomic planner by [6] which is based on Reeds and Shepp's curves made up with arc of circle and line segments. The curvature discontinuity occuring between an arc of circle and a line segment (or two arcs) obliges the vehicle to move away from the reference path. This phenomenon can be strongly reduced if the robot's acceleration is controlled instead of its velocity.

Another important hypothesis, implicitly made in those works, is that the robot's configuration is assumed to be perfectly known at each time. This last assumption is known by roboticians to be very unrealistic. Contrary to manipulators whose basis remains fixed with respect to the reference frame, and for which the position of end effector may be directly deduced from the measure of the angles between successive links, mobile robots may drift during their motion and their exact position cannot be known using dead reckononing techniques only. For this reason exteroceptive measurements *must* be processed to update the vehicle localization in order to limit the estimation error. Estimation of robot localization has received much interest [7], [8] and [9]. But the fact is that, even by merging the information provided by several sensors, the robot's configuration is obtained with some errors which *cannot* be neglected.

This paper addresses the problem of determining a feedback control law, robust with respect to localization and curvature estimation errors, allowing a mobile robot to follow a prescribed path. The model we consider is a dynamic extension of the usual kinematic model of a car-like robot in the sense that we define the curvature as a new state variable. The control variable are respectively the linear velocity and the derivative of the curvature.

By means of sliding mode techniques combined with Lyapunov analysis we determine a stabilizing controller for the system when the state is supposed to be perfectly known. Then, we prove that the system remains stable when the estimated state values are considered instead of the exact

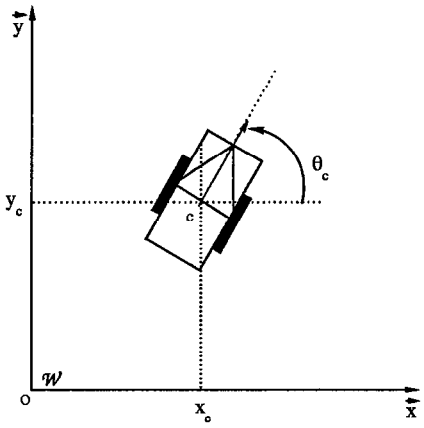


Figure 1: Vehicle configuration

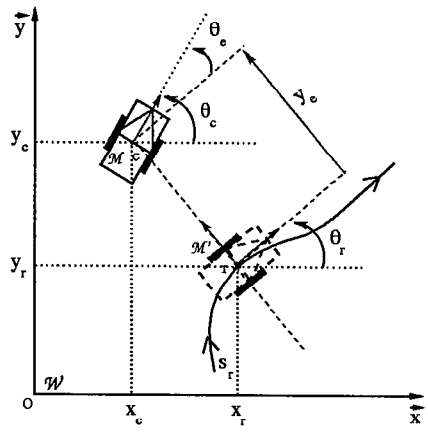


Figure 2: Path following

ones. The robustness property is then expressed by determining, around each point of the nominal trajectory, a bounded attractive domain where the vehicle's configuration could possibly lie, as the feedback control is performed according to estimation errors.

These techniques have been successfully applied to design a robust path following controller for a mobile platform ROBUTER$^{TM}$; experimental results are presented at the end of the paper.

The paper is organized as follows: The problem is stated in section 2. First, we describe the vehicle's kinematics, and we state the path following control problem for our model (§ 2.1 and § 2.2). Then we introduce the robustness problem and we modelize the localization and orientation error (§ 2.3). Section 3 describes the controller. The stability is first analyzed for the nominal case (§ 3.1). Then the robustness is described by computing the attractive domain (§ 3.2) when estimated values are considered. Finally, an account of experimental results is given in the last section (§ 4).

# 2 Problem statement

The definition of robustness for tracking control naturally stems from both the statement of the tracking control (sec. § 2.2) and the description of the vehicle kinematics (sec. § 2.3).

## 2.1 Vehicle's kinematics

The model of a car-like robot is represented by figure 1. A configuration of the car is described by a vector $P_c = (x_c, y_c, \theta_c)^T$ where $(x_c, y_c)$ are the coordinates of a reference point $c$ with respect to the world frame $\mathcal{W}$ and the angle $\theta_c \in S^1$ represents the direction of the car with respect to the $x$-axis.

The robot's kinematic is described by (1)

$$\dot{P}_c(t) = \begin{cases} \dot{x}_c &= v_c \cos\theta_c \\ \dot{y}_c &= v_c \sin\theta_c \\ \dot{\theta}_c &= \omega_c = v_c \chi_c \end{cases} \quad (1)$$

The control inputs $(v_c(t), \omega_c(t))^T$ respectively stand for the linear and angular velocities of the car. In the sequel we consider a dynamic extension of this system.

## 2.2 Path following control

Several studies on modeling and control of wheeled robots have been realized and experimented (See [10], [11] and [5]). The approach we have chosen to follow here, is the one described in [5], presented in this section as a particular case of the tracking control problem [12]. The parameterization described in [5] is defined by means of a Frenet frame $\mathcal{M}'$ whose origin "$r$" is the projection of the robot's reference point "$c$" on the path at each time, see figure 2.

The path following problem consists of finding a control law insuring a geometrical convergence towards the path to be followed regardless to the translational velocity $v_c$ of the robot. Assuming that $\mathcal{M}'$ is the frame of a kinematically equivalent fictitious robot, the error configuration vector $P_e$ with respect to $\mathcal{M}'$ is then:

$$\begin{cases} P_e = P_e^{\mathcal{M}'} = TP_e^{\mathcal{W}} = T(P_c - P_r); \\ T = \begin{pmatrix} \cos\theta_r & \sin\theta_r & 0 \\ -\sin\theta_r & \cos\theta_r & 0 \\ 0 & 0 & 1 \end{pmatrix} \end{cases} \quad (2)$$

The time derivative of the configuration error is defined by (3):

$$\begin{pmatrix} \dot{x}_e \\ \dot{y}_e \\ \dot{\theta}_e \end{pmatrix} = \begin{pmatrix} v_r\chi_r y_e - v_r + v_c\cos\theta_e \\ -v_r\chi_r x_e + v_c\sin\theta_e \\ v_c\chi_c - v_r\chi_r \end{pmatrix} \quad (3)$$

In this expression, $\chi_r = \omega_r / v_r$ and $\chi_c = \omega_c / v_c$ define respectively the curvature of the reference path and the curvature of the path realized by the robot; $v_r$ and $v_c$ represent respectively the linear velocity of the reference vehicle and the linear velocity of the robot.

As the fictitious robot is defined by the orthogonal projection of the robot on the reference path, the first error coordinate $x_e$ and its derivative $\dot{x}_e$ remain equal to zero as the robot moves. Therefore, from the first equation of (3) we have:

$$v_r = \frac{v_c \cos\theta_e}{1 - \chi_r y_e} \text{ under the constraint } [1](1 - \chi_r y_e) > 0 \tag{4}$$

Introducing the arclength abscissa $s_r$ along the reference path as a new state variable, kinematic equations of system (3) can be rewritten as:

$$\begin{cases} \dot{s}_r &= \frac{v_c \cos\theta_e}{1-\chi_r y_e} \\ \dot{y}_e &= v_c \sin\theta_e \\ \dot{\theta}_e &= v_c \chi_e \end{cases} \tag{5}$$

where $\chi_e = \chi_c - \chi_r^r$ and $\chi_r^r = \chi_r \frac{\cos\theta_e}{1-\chi_r y_e}$.

Now, in order to take into account the inertia of actuators we propose to consider a dynamic extension of (5). As explained in the introduction this extension will allow the robot to remain close to the trajectory when the reference path's curvature is discontinuous.

The dynamic extension is defined as follows:

$$\begin{cases} \dot{s}_r &= \frac{v_c \cos\theta_e}{1-\chi_r y_e} \\ \dot{y}_e &= v_c \sin\theta_e \\ \dot{\theta}_e &= v_c \chi_e \\ \dot{\chi}_e &= u_c - \dot{\chi}_r^r \end{cases} \tag{6}$$

where $\chi_e$ is now viewed as state variable and $(v_c, u_c)$ constitute the new vehicle's control inputs for the path following process.

## 2.3 Robustness problem

As stated in the introduction, the current configuration on the robot as well as the instantaneous curvature are not directly measurable. Therefore, the real inputs of the feedback control are the estimated values $(\hat{P}_e^T, \hat{\chi}_e)$ instead of the true ones:

$$\hat{u}_c = u_c(\hat{P}_e^T, \hat{\chi}_e) \tag{7}$$

Estimates $\hat{P}_e$ of $P_e$ (2) and $\hat{\chi}_e$ of $\chi_e$ (3) are obtained from the estimates $(\hat{P}_c = P_c + \delta P_c, \hat{\chi}_c = \chi_c + \delta\chi_c)$ of both the configuration and the curvature, continuously updated by combining deadrekoning and exteroceptive measurements (See [8] and [13]. These estimates lie in a compact confidence domain centered around $(\hat{P}_c, \hat{\chi}_c)$ (see Figure 3) $(\hat{P}_c = P_c + \delta P_c;\ \delta P_c \in \Omega)$.

[1] This condition, means that the orthogonal projection of the point $c$ on the reference path exists and it is unique (see Samson, 1992 for details).

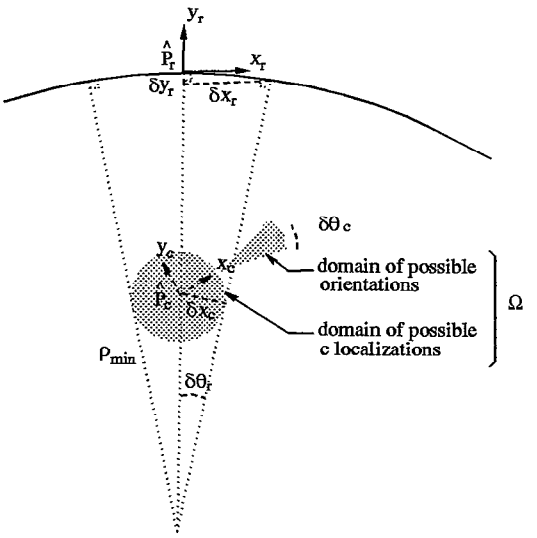


Figure 3: Path following

By virtue of EKF formalism [14] or merely for computational ease [9], the feasible domain $\Omega$ is described as an ellipsoid, a truncated cylinder or a bounding box.

In contrast to the tracking control problem where errors on the vehicle localization do not modify the target vehicle's configuration, it is clear from figure 3 that inaccuracy on the vehicle's localization induces an error on the Frenet frame localization in which the variations are defined. Indeed, this frame is obtained by projecting on the nominal curve the set of uncertain[2] localization of the characteristic point $P_c$. If we suppose that $1 - \hat{\chi}_r \hat{y}_e > 0$, then $\forall \delta P_c \in \Omega$, an approximated value of $\delta P_r$ can be deduced geometrically (see figure 3)

$$\begin{cases} \delta\theta_r &= \text{asin}\frac{\delta x_c}{\rho_{min} - y_e} \\ \delta x_r &= \rho_{min} \sin(\delta\theta_r) \\ \delta y_r &= \delta x_r \sin\delta\theta_r \end{cases} \tag{8}$$

Taking into account these new inaccuracys, under the assumption that $(1 - \hat{\chi}_r \hat{y}_e >> 0)$ and $\delta\chi_c \in \mathcal{X} = [-\delta\chi_{max}, \delta\chi_{max}]$ and following (2) we get:

$$\begin{cases} \hat{P}_e &= \hat{T}(\hat{P}_c - \hat{P}_r) = P_e + \delta P_e \\ \hat{\chi}_e &= \hat{\chi}_c - \hat{\chi}_r^r = \chi_e - \delta\chi_e \end{cases} \tag{9}$$

where, from (9) and (2):

$$\delta P_e = \begin{cases} \delta x_e &= \cos\hat{\theta}_r(\delta x_c - \delta x_r) + \sin\hat{\theta}_r(\delta y_c \\ &\quad -\delta y_r) - \delta\theta_r y_e \\ \delta y_e &= -\sin\hat{\theta}_r(\delta x_c - \delta x_r) + \cos\hat{\theta}_r(\delta y_c \\ &\quad -\delta y_r) \\ \delta\theta_e &= \delta\theta_c - \delta\theta_r \end{cases} \tag{10}$$

In the sequel, the value of $\delta x_e$ will be of no importance as the path following problem only involves the variation

[2] for simplicity, the feasible domain $\Omega$ is regarded as a truncated cylinder with flat circular ends containing the domain updated by EKF

of $y_e$ and $\theta_e$. It is worth noting that $\delta y_e$ is just the second element of a rotation of $(\delta P_c - \delta P_r)$.

From the control point of view, the investigated robustness problem can be stated as follows:

*Consider the feedback control law (7) with the estimate $(\hat{P}_c^T, \hat{\chi}_c)$ as input instead of the true value $(P_c^T, \chi_c)$. Is the equilibrium point of system (3) with the uncertain control law (7) still stable under the assumption that the estimation error $(\delta P_c^T, \delta\chi_c)$ lies in an a priori known bounded domain $(\Omega, \mathcal{X})$?*

*Moreover, if the stability is proven, what is the precision of the regulation i.e. what is the size of the attractive domain containing $(P_e^T, \chi_e) = 0$?*

We answer this question in the next section via stability analysis by combining *sliding surface* with the use of an appropriate *Lyapunov function.*

# 3 Robust dynamic state feedback controller

In this section we design the path following control by determining an appropriate sliding surface ($z_e = 0$), defined by:

$$z_e = y_e + \lambda \text{sign}(v_c)\theta_e + \mu\chi_e, \quad \lambda, \mu > 0 \qquad (11)$$

We are going to prove, in the sequel, that the convergence of $y_e, \theta_e$ and $\chi_e$ to zero can be insured once the state space is reduced to the surface $z_e = 0$. First, to guarantee the convergence of $z_e$ to zero we impose the following dynamics on the variable $z_e$:

$$\dot{z}_e = -|v_c|\frac{k}{\lambda}z_e, \quad k > 0 \qquad (12)$$

the control law $u_c$ becomes:

$$u_c = \dot{\chi}_r^r - \frac{|v_c|}{\mu}[\text{sign}(v_c)\sin\theta_e + \lambda\chi_e + \frac{k}{\lambda}z_e] \qquad (13)$$

## 3.1 Stability

Now, in the aim of proving the stability of system (3) under control (13), we introduce the following Lyapunov function:

$$V(P_e^T, \chi_e) = \frac{\lambda}{2}[kz_e^2 + \lambda^2\mu\chi_e^2 + 4\lambda^2\sin^2(\frac{\theta_e}{2})] \qquad (14)$$

Using (3) and (13) the time derivative of $V$ can be expressed as follows:

$$\dot{V}(P_e^T, \chi_e) = -\mid v_c \mid [k^2 z_e^2 + \lambda^2 k\chi_e z_e + \lambda^4\chi_e^2] \qquad (15)$$

As $\dot{V}(P_e^T, \chi_e)$ is a semi-definite negative function, and as the set of points $\{z_e = \chi_e = 0,\ y_e = -\lambda\text{sign}(v_c)\theta_e\}$ over which $\dot{V}$ vanishes (under the hypothesis that $v_c$ does not converges to zero) constitutes an invariant set for system (6), we know from La Salle's theorem that any trajectory starting from a well defined bounded region will converge to this set:

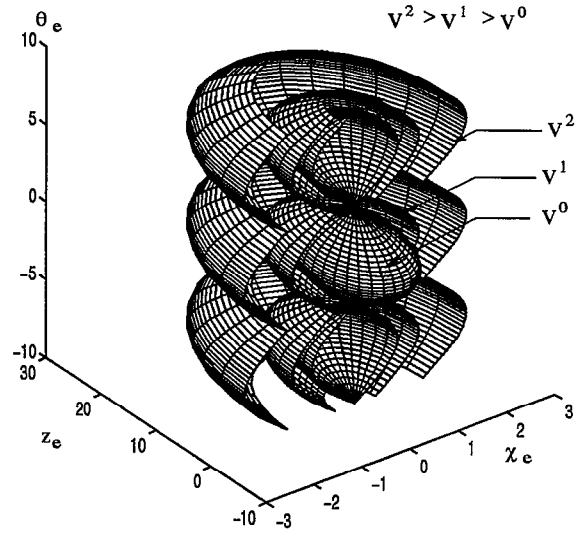


Figure 4: Domain of stability

Furthermore, as $y_e = -\lambda\text{sign}(v_c)$ once $z_e = 0$, the dynamics of $y_e$ given by (6) becomes:

$$\dot{y}_e = -|v_c|\sin\frac{y_e}{\lambda}$$

Therefore, paths starting from the region where $z_e = \chi_e = 0$ and $|y_e| < \lambda\pi$, will converge to the origin point $x_e = y_e = \theta_e = \chi_e = 0$.

Now, the remaining question we need to answer is: *how to ensure that the representative point controlled by (13) will reach the manifold $z_e = \chi_e = 0$ within the region where $|y_e| < \lambda\pi$?*

This question can simply be answered by considering the Lyapunov function (14). From figure(4), where several contour surfaces of $V$ are represented. It appears that there exists a value $V^0$ (one can verify easily that $V^0 = V(0, 0, (2n+1)\pi) = 2\lambda^3$) such that the set of point $(P_e, \chi_e)$ verifying $V(P_e, \chi_e) \leq V^0$ is the infinite union of compacts sets connected to one another by a unique point on the $\theta$-axis. Therefore, the domain $\mathcal{S} = \{(P_e, \chi_e)/V(P_e, \chi_e) < V^0, \theta_e \in ]-\pi, \pi[, 1 - \chi_r y_e > 0\}$ defines an open neighborhood of the origin point $(P_e = 0, \chi_e = 0)$. Now, as $V$ is a decreasing function of the state, if a trajectory starts inside the domain $\mathcal{S}$, the representative point converges to the unique equilibrium point, $(P_e = 0, \chi_e = 0)$. Note that, depending on the initial conditions, the gains $\lambda, \mu$ and $k$ can be chosen so that the initial point belongs to $\mathcal{S}$, insuring the convergence of the corresponding trajectory to zero. A practical computation of the set $\mathcal{S}$ can be

obtained following the same method as the one developed in [12] this is done in Appendix.

## 3.2 Robustness

In this section, we state in a more precise way the robustness problem in the state space of points $(P_e, \chi_e)$. We will say that the closed-loop controller is robust (with respect to localization errors and curvature estimation) if the path following can still be achieved when the estimated values are considered instead of the exact ones. More precisely, suppose that we have determined a Lyapunov function $V(P_e, \chi_e)$, and a region $S$ of the $(P_e, \chi_e)-$space, such that: $\forall (P_e, \chi_e) \in S$ the Lyapunov function decreases in the nominal case (i.e. when exact state values are considered). Now, is it possible to determine a compact domain $\mathcal{A}(\Omega, \mathcal{X}) \subset S$ such that: $\exists\ \gamma(\Omega, \mathcal{X}) > 0 \mid \forall (\delta P_c, \delta\chi_c) \in \Omega \times \mathcal{X}$, and $\forall (P_e, \chi_e) \in S \setminus \mathcal{A}(\Omega, \mathcal{X})$,

$$V(P_e, \chi_e) \geq \gamma(\Omega, \mathcal{X}) \Rightarrow \dot{V}(\hat{P}_e, \hat{\chi}_e) < 0 \qquad (16)$$

In other terms $\mathcal{A}(\Omega, \mathcal{X})$ is defined as a contour surface of $V$ outside which the Lyapunov function decreases. In the case that such a set $\mathcal{A}(\Omega, \mathcal{X})$ is determined, the path following control law is said to be *robust* against configuration inaccuracy ($\hat{P}_c = P_c + \delta P_c$) and curvature estimation ($\hat{\chi}_c = \chi_c + \delta\hat{\chi}_c$), according to the notation introduced at section 2.3.

Now, let us go back to system (6) and consider the closed-loop control (7) with the estimated state values instead of the exact ones. We get:

$$\left\{ \begin{array}{rcl} \dot{s}_r & = & \frac{v_c \cos\theta_e}{1 - x_r y_e} \\ \dot{y}_e & = & v_c \sin\theta_e \\ \dot{\theta}_e & = & v_c \chi_e \\ \dot{\chi}_e & = & \hat{u}_c - \dot{\chi}_r^r \end{array} \right. \qquad (17)$$

$$\text{with} \quad \hat{u}_c = \dot{\hat{\chi}}_r^r - \frac{|v_c|}{\mu}[\text{sign}(v_c)\sin\hat{\theta}_e + \lambda\hat{\chi}_e + \frac{k}{\lambda}\hat{z}_e] \quad (18)$$

and $\hat{\theta}_e = \theta_e + \delta\theta_e$, $\hat{\chi}_e = \chi_e + \delta\chi_e$, $z_e = z_e + \delta z_e$ and $\dot{\hat{\chi}}_r^r = \dot{\chi}_r^r + \delta\dot{\chi}_r^r$. Under the hypothesis that the error $\delta\theta_e$ is small enough, we consider the following first order approximation: $\sin\hat{\theta}_e = \sin\theta_e + \delta\theta_e \cos\theta_e$.

Using this expression in (18) we get:

$$\dot{\chi}_e = -\frac{|v_c|}{\mu}([\text{sign}(v_c)\sin\theta_e + \lambda\chi_e + \frac{k}{\lambda}z_e] - \epsilon) \quad (19)$$

where $\epsilon$ represents the error term:

$$\begin{array}{rcl} \epsilon & = & \text{sign}(v_c)\delta\theta_e \cos\theta_e + \lambda\delta\chi_e + \frac{k}{\lambda}(\delta y_e + \lambda\text{sign}(V_c)\delta\theta_e \\ & & +\mu\delta\chi_e) - \frac{\mu}{|v_c|}\delta\dot{\chi}_r^r \end{array} \qquad (20)$$

Using the estimated values, the dynamics of $z_e$ (given by (12) in the nominal case) turns out to be:

$$\dot{z}_e = -|v_c|(\frac{k}{\lambda}z_e + \epsilon) \qquad (21)$$

Now, in order to prove that the representative point converges towards an attractive domain let us consider the Lyapunov function (14) anew, and compute its time derivative with respect to the dynamics of system (17):

$$\begin{array}{rcl} \dot{V} & = & -\frac{|v_c|}{2}(k^2 z_e^2 + k\lambda z_e\epsilon + \lambda^4\chi_c^2 + \lambda^2 k z_e\chi_e + \lambda^3\chi_e\epsilon) \\ & = & -\frac{|v_c|}{2}(X^T\Sigma X - H) \end{array}$$

where $X = (z_e + \frac{\lambda\epsilon}{3k}, \lambda\chi_e + \frac{\epsilon}{3})$, $\Sigma = \begin{pmatrix} k^2 & \frac{\lambda k}{2} \\ \frac{\lambda k}{2} & \lambda^2 \end{pmatrix}$ and $H = \frac{\lambda^2\epsilon^2}{3}$

### 3.2.1 Computation of the attractive domain $\mathcal{A}(\Omega, \mathcal{X})$

From this last expression, the set of point verifying $\dot{V} = 0$ may be viewed as the contour curve corresponding to the value $H$ for the Riemannian distance defined by the definite positive matrix $\Sigma$ in the $(z_e, \chi_e)-$plane, with respect to the new frame centered at $(-\frac{\lambda\epsilon}{3k}, -\frac{\epsilon}{3})$ and whose basis is obtained by keeping the same unit vector along the $z_e$-axis and by multiplying by $1/\lambda$ the unit vector along the $\chi_e$ axis. Depending on the sign of $\epsilon$, the set of points verifying $\dot{V} = 0$ defines two symmetric ellipses with respect to the origin, see figure 5. From this representation we know that $\dot{V} < 0$ for $X^T\Sigma X > H$, i.e. outside the contour curve $\dot{V} = 0$

Using Lagrange multipliers we can simply compute the extremal values of $z_e$ and $\chi_e$ along the contour curve $\dot{V} = 0$.

Considering the augmented function $G_{z_e} = z_e + m\dot{V}$, $m \in \mathbf{R}$ and writing that $\frac{\partial G_{z_e}}{\partial\chi_e} = \frac{\partial G_{z_e}}{\partial z_e} = 0$, we deduce that extremal values of $z_e$ are obtained for: $\chi_e = -\frac{kz_e + \lambda\epsilon}{2\lambda^2}$. Replacing this last expression in equation $\dot{V} = 0$ we obtain:

- $-\frac{\lambda\epsilon}{k} \leq z_e \leq \frac{\lambda\epsilon}{3k}$ when $\epsilon > 0$,
- $\frac{\lambda\epsilon}{3k} \leq z_e \leq -\frac{\lambda\epsilon}{k}$ when $\epsilon < 0$

Note that $\chi_e = 0$ when $z_e = -\frac{\lambda\epsilon}{k}$, and $\chi_e = -\frac{2\epsilon}{3\lambda}$ when $z_e = \frac{\lambda\epsilon}{3k}$.

Using a same reasoning with the augmented function $G_{\chi_e} = \chi_e + m\dot{V}$, $m \in \mathbf{R}$ we get:

- $-\frac{\epsilon}{\lambda} \leq \chi_e \leq \frac{\epsilon}{3\lambda}$ when $\epsilon < 0$,
- $\frac{\epsilon}{3\lambda} \leq z_e \leq -\frac{\epsilon}{\lambda}$ when $\epsilon > 0$

$z_e = 0$ when $\chi_e = -\frac{\epsilon}{\lambda}$, and $z_e = -\frac{\epsilon}{3k}$ when $\chi_e = \frac{\epsilon}{3\lambda}$.

This construction achieves to characterize the projection of the equipotential curve $\dot{V} = 0$ in the $(z_e, \chi_e)$-plane.

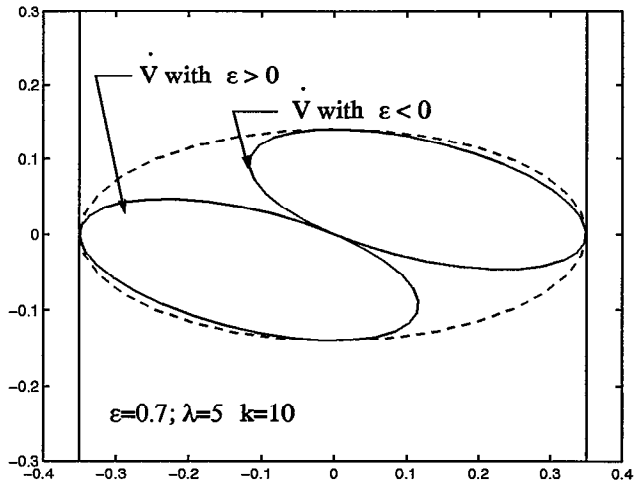


Figure 5: The attractive domain in the $(z_e, \chi_e)-$ plane

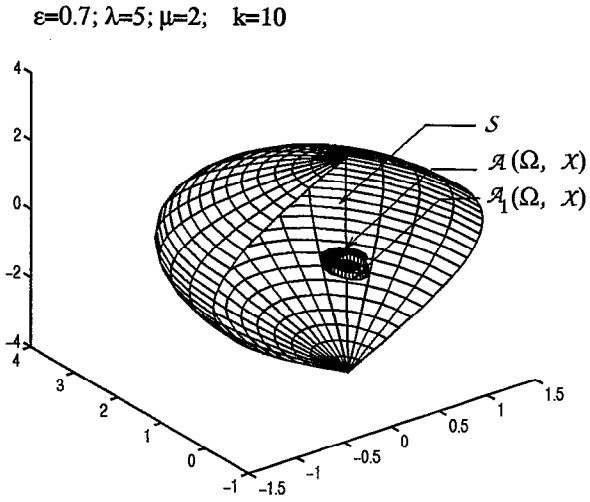


Figure 6: The attractive domain in $\mathcal{A}_1(\Omega, \mathcal{X})$

Now, in order to compute the attractive set we need to bound the two other state variables, $y_e$ and $\theta_e$. To compute these bounds easier we are going to consider a convex hull of the two ellipsoids obtained for $\epsilon > 0$, and $\epsilon < 0$. Let us consider the ellipse centered at the origin ($z_e = 0, \chi_e = 0$), whose equation is given by:

$$\frac{1}{\lambda^2} z_e^2 + \frac{\lambda^2}{k^2} \chi_e^2 = \frac{\epsilon^2}{k^2} \tag{22}$$

This ellipse is tangent to the previous two ellipses ($\epsilon > 0$ or $\epsilon < 0$): vertically at the points ($z_e = \frac{\lambda\epsilon}{3k}, \chi_e = 0$) and horizontally at the points ($z_e = 0, \chi_e = -\frac{\epsilon}{\lambda}$). It is the smallest ellipse centered at the origin, with vertical and horizontal axis and containing the two ellipsoids. Therefore, it constitutes a good approximation of their union (see figure 5).

Using this approximation, we can now easily determine bounds on the remaining two state variables as follows. As $z_e = y_e + \lambda\theta_e sign(v_c) + \mu\chi_e$,

$$\theta_e = -\left(\frac{y_e - [z_e - \mu\chi_e]}{\lambda}\right) sign(v_c) \tag{23}$$

Therefore the dynamics of $y_e$ given by (17) becomes:

$$\dot{y}_e = -|v_c| \sin\left(\frac{y_e - [z_e - \mu\chi_e]}{\lambda}\right) \tag{24}$$

and then, so long as $|y_e| < |z_e - \mu\chi_e|$, $|y_e|$ decreases. To compute a bound for $y_e$ let us look for the maximum value of $z_e - \mu\chi_e$ over the ellipse (22). Once more we use Lagrange multipliers:

Consider the augmented function:

$G_{(z_e-\mu\chi_e)} = z_e - \mu\chi_e + m(\frac{z_e^2}{\lambda^2} + \frac{\lambda^2\chi_e^2}{k^2} - \frac{\epsilon^2}{k^2})$

Writing that $\frac{\partial G_{(z_e-\mu\chi_e)}}{\partial z_e} = \frac{\partial G_{(z_e-\mu\chi_e)}}{\partial \chi} = 0$.

we get $\chi_e = -\frac{\mu k^2 z_e}{\lambda^4}$; replacing this expression in equation (22) it comes:

$$z_e = \pm\frac{\lambda^3\epsilon}{k\sqrt{\lambda^4 + \mu^2 k^2}}, \quad \chi = \pm\frac{\epsilon\mu k}{\lambda\sqrt{\lambda^4 + \mu^2 k^2}} \tag{25}$$

The maximum value of $|z_e - \mu\chi_e|$ is then obtained when the signs of $z_e$ and $\chi$ are opposite:

$$\text{Max } |z_e - \mu\chi_e| = \frac{|\epsilon|(\lambda^4 + \mu k^2)}{k\lambda\sqrt{\lambda^4 + \mu^2 k^2}} = Y \tag{26}$$

Therefore, so long as $|y_e| > Y$, $|y_e|$ decreases.

Now, as $\theta_e = \frac{z_e - \mu\chi_e - y_e}{\lambda}$ the bound on $\theta_e$ can be deduced as follows:

$$|\theta_e| \leq \frac{2Y}{\lambda} = \Theta \tag{27}$$

This last bound achieves the characterization of the domain of attraction as the set of points $(\chi_e, y_e, \theta_e)$ in $\mathbf{R}^3$ defined by:

$$\mathcal{A}_1(\Omega, \mathcal{X}) = \{(y_e, \theta_e, \chi_e) \in [-Y, Y] \times [-\Theta, \Theta] \times \mathbf{R}, \text{ such that } \frac{z_e^2}{\lambda^2} + \frac{\lambda^2\chi_e^2}{k^2} - \frac{\epsilon^2}{k^2} \leq 0\} \tag{28}$$

If we want to determine it by means of the definition stated at the beginning of section3.2, the attractive domain $\mathcal{A}(\Omega, \mathcal{X})$ is given by the smallest equipotential of $V$ surrounding $\mathcal{A}_1(\Omega, \mathcal{X})$. It must be noticed that this latter definition of $\mathcal{A}(\Omega, \mathcal{X})$ provides a very pessimistic representation of the actual attractive domain (see figure 6).

### 3.2.2 Utility of $\mathcal{A}(\Omega, \mathcal{X})$

The precision specification is of great utility to design safe path following process. Indeed, it can be used to define practical collision-free path when they are realized in closed loop form, i.e *if we assume the inaccuracy domains $\Omega$ and $\mathcal{X}$ to be a priori known, the path is said to be achievable if, for any configuration taken on the perturbed path with control unprecsion $\mathcal{A}_1(\Omega, \mathcal{X})$, the vehicle does not intersect obstacles*. Figure 7-a, presents a real situation (a vehicle in a corridor). The uncertain localization set $\Omega$ considered here is a truncated cylinder (half-height $\delta\theta_c = 0.05rd$ and radius $\delta x_c(\delta y_c) = 0.15m$) centered around the estimated configuration (we have fixed $\mathcal{X} = [-0.01m^{-1}, 0.01m^{-1}]$). One notices that, along the line segment, the vehicle may collide with obstacles because the projection of $\mathcal{A}_1(\Omega, \mathcal{X})$ on the $(y_e, \theta_e)-$plane is given by $y_e = 0.9m$ and $\theta_e = 0.36rd$ (see figure 7-b). In this case, the planned path through the corridor appears to be no safe. Changing the values of the controller's gains (see figure 7-c) the robot's trajectory does not collide with obstacles anymore (the projection of $\mathcal{A}_1(\Omega, \mathcal{X})$ on $y_e, \theta_e$-plane is given by $y_e = 0.27m$ and $\theta_e = 0.08rd$).

In conclusion, if one wants the vehicle to achieve safely a mission, the size of the attractive domain $\mathcal{A}_1(\Omega, \mathcal{X})$ (or $\mathcal{A}(\Omega, \mathcal{X})$) has to be minimized under the constraint that a judicious balance between response time, no output oscillation, robustness and the size of the stability domain $\mathcal{S}$ has to be found.

# 4 Experimental results

The proposed controller has been implemented on a ROBUTER$^{TM}$ (Figure 8) using the VxWorks Real-time kernel.

Three classes of experiments are shown in the sequel. Each class contains two experiments and corresponds to a specific choice of the controller gain $k$ (we have set $\lambda = 5$, $\mu = 2$ for all the experiments). In each case, the vehicle has to follow a 9 meters-long path successively made up with a line segment, three arcs of circle and a final line segment as shown on figure 9. This trajectory represents the output of a typical path planner. Initial configuration and curvature errors are $(\hat{P}_e^T(0), \hat{\chi}_e(0)) \simeq (0, 2cm, \frac{\pi}{6}rd, 0)$.

During these experiments, a constant speed of $20cms^{-1}$ was maintained for the vehicle along the path. The sampling time ($T_e$) of the controller was fixed equal to $0.6s$. During $T_e$ the mobile robot's localization is continuously updated by integrating the wheels rotation angle (odometry) and, when available, by exteroceptive (telemetric) measurements. Computations are processed with Extended Kalman Filtering and yield a configuration estimation $\hat{P}_c(t)$ with uncertainty characterization $\Omega(t)$. The curvature estimation is updated at each period by using the orientation

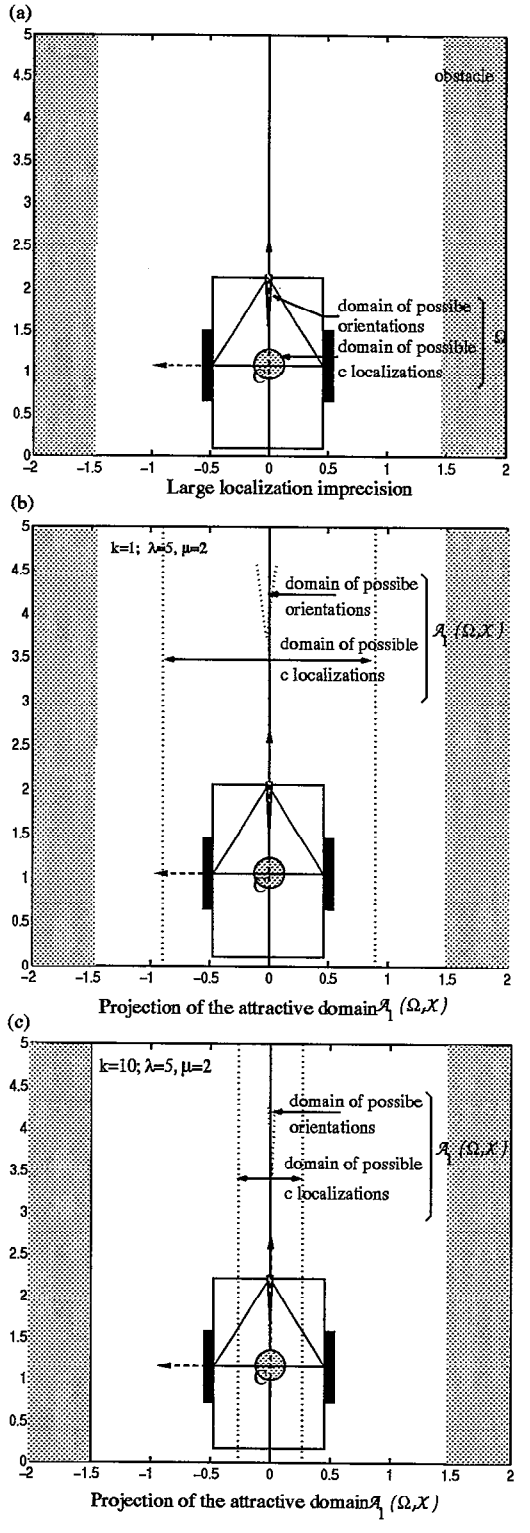


Figure 7: Projection of $\mathcal{A}(\Omega, \mathcal{X})$ along the planned path

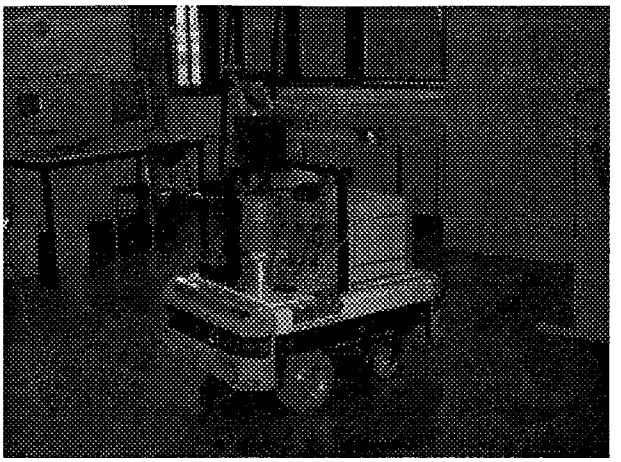

Figure 8: The ROMO Sapiens robot

estimates produced by the localization procedure:

$$\hat{\chi}_c^{t'} = \frac{\hat{\theta}_c^{t'} - \hat{\theta}_c^t}{v_c T_e} \quad \text{where } (t' = t + T_e)$$

Results are shown on figure 10 where the boxes represent the configuration estimation of the vehicle, the ellipses represent the confidence domain of the position estimations, obstacles are represented by broken-lines.

We remark that when the gain $k = 1$, the robot runs into the obstacles. This experiment corroborates what already we said in section concerning the choice of the gain and the size of the attractive domain. In the case where $k = 3$, the robot achieves his mission but with a great inaccuracy. Finally for $k = 10$, in the last experiment, the task has been performed in a very satisfactory way: the path performed by the robot merges practically with the planned one.

# 5 Conclusion

The precise determination of an attractive domain around each point of the reference path, where the robot could possibly lie during the closed-loop path following process, constitutes a new useful result for planning safe trajectories.

Indeed, whereas previous works have considered the propagation of estimation errors to design safe open-loop trajectories (see the work in [15] such an approach did not allow to analyze the robustness of feedback controller with respect to localization errors. However, as wheeled robots may drift during their motion the question of designing robust control laws to achieve stabilization process appears to be essential.

In the anterior work in [12] such an attractive domain was characterized by means of a Lyapunov function. This set was delimited by an equipotential surface, and its computation required a time-consuming optimization process.

Here, by determining an explicit formulation of $\mathcal{A}_1(\Omega, \mathcal{X})$ we get a very simple tool to compute the attractive region along the path. Furthermore, the two-steps reasoning analyzing first the convergence to the surface $z_e = 0$ allows to specify smaller bounds on the state variables making the result more precise.

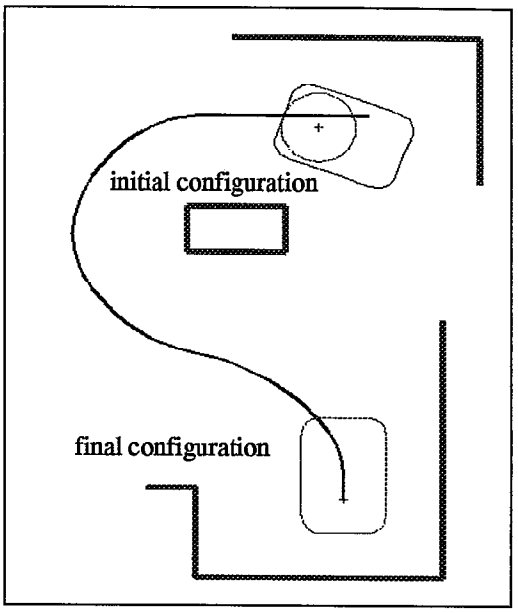


Figure 9: "Experimental result" The planned path for the ROBUTER$^{TM}$

Our theoretical robustness result has been confirmed by several experiments made on a mobile platform ROBUTER$^{TM}$. Tuning up the gains to minimize the size of the attracive domain under the constraint to balance between short response time, low output oscillation, robustness and large stability domain, appears to be the central question. We think that the design of a Variable Structure Control upon the sliding surface $z_e = 0$ could make this latter point easier; we are actually working on it.

# References


[1] C. Canudas, H. Khennouf, C. Samson, and O. J. Sordalen, *Nonlinear Control Design for Mobile Robots.* to appear in the book on Mobile Robots World Scientific Publisher,(Zheng, editor), 1994.

[2] M. Tounsi, G. Lebert, and M. Gautier, "Dynamic control of nonholonomic mobile robot in cartesian space," in *Proceedings IEEE Conference on Decision and Control, Louisianne*, 1995.

[3] B. Thuilot, "Contribution à la modélisation et à la commande de robots mobiles à roues," *PhD thesis, Ecoles des Mines de Paris, december*, 1994.

[4] C. Samson and Aït-Abderrahim, "Feedback Control of a Nonholonomic Wheeled Cart in Cartesian Space," in *Proceedings of the IEEE Int. Conf.*

*Robotics and Automation R&A'91*, pp. 1136–1141, 1991.

[5] C. Samson, "Path following and time-varying feedback stabilization of a wheeled mobile robot," in *Proceedings of ICARCV'92 , Singapore, sept*, pp. RO–13.1.1–RO–13.1.5, 1992.

[6] J.-P. Laumond, P. Jacobs, M. Taïx, and R. Murray, "A motion planner for nonholonomic mobile robots," *IEEE Transactions on Robotics & Automation*, vol. 10, no. 5, 1994.

[7] T. Hamel, E. Halbwachs, and D. Meizel, "La Géometrie offre t-elle une Alternative au Filtrage de Kalman ?," in *Proceedings of the SEE nat. Conf. Localisation En Robotique , Supélec, Gif sur Yvette, France*, pp. 53–61, 1993.

[8] J. J. Leonard and H. Durrant-Whyte, "Mobile Robot Localization by Tracking Geometric Beacons," *IEEE Transactions on Robotics & Automation*, vol. 7, no. 3, pp. 376–382, 1991.

[9] A. Preciado, D. Meizel, A. Segovia, and M. Rombaut, "Fusion of Multi-Sensor Data: a Geometric Approach," in *Proceedings of the IEEE Int. Conf. Robotics and Automation R&A'91*, pp. 2806–2811, 1991.

[10] W. L. Nelson and I. J. Cox, "Local path control for autonomous vehicle," in *Proceedings of the IEEE Int. Conf. Robotics and Automation R&A'88,Philadelphia, Pennsylvania*, pp. 1504–1510, 1988.

[11] O. J. Sordalen, "Feedback control of nonholonomic mobile robots, departement of engineering cybernetics, the norwegen institute of technology," vol. 93-5-W, 1993.

[12] T. Hamel and D. Meizel, "Robust control laws for wheeled mobile robots," *International Journal of Systems Science*, vol. 27, no. 8, pp. 695–704, 1996.

[13] C. Durieu, M. J. Aldon, and D. Meizel, "Multisensory data fusion for localisation in mobile robotics," *Revue de traitement du signal*, vol. 13, no. 12, pp. 143–165, 1996.

[14] P. Cheesman and R. C. Smith, "On the representation and estimation of spatial uncertainty," *International Journal of Robotics Research*, vol. 5, no. 4, pp. 56–68, 1986.

[15] T. Siméon and R. Alami, "Planning robust motion strategies for a mobile robot in a polygonal world," *Revue d'intelligence artificielle*, vol. 8, no. 4, pp. 383–401, 1994.

# Appendix

*Computation of the stability domain $\mathcal{S}$*

Reconsidering the definition of $\mathcal{S}$ given in section 3.1, it must be noted that, in practice, the computation of the convergence domain $\mathcal{S}$, as defined, is not an easy task. However, if we consider $|y_e| < \frac{1}{\chi_{r_{max}}}$ and assuming that:

$$\forall (y_e, \theta_e, \chi_e) \in \mathbf{R}\times ]-\pi, \pi[\times \mathbf{R},\ V(P_e(0), \chi_e(0)) < \mathrm{Min}(2\lambda^3, \tfrac{1}{2}k\lambda\tfrac{1}{\chi^2_{r_{max}}}),$$

then control (13) asymptotically stabilizes $(y_e, \theta_e, \chi_e)$ at the origin. In the sequel we prove that the configuration and curvature errors converge to zero.

- the case that $2\lambda^3 < \frac{1}{2}k\lambda$ presents no problem,
- in the adverse case, we can easily shown that the maximum of $z_e$ on the contour curve:

  $$V(P_e, \chi_e) - V(P_e(0), \chi_e(0))$$

  is given when $\chi_e = \theta_e = 0$. Hence $z_e^{max} = y_e$. However, as we want $|y_e|$ to remain inferior to $\frac{1}{\chi_{r_{max}}}$, it suffice to take $V(P_e, \chi_e) < \frac{k\lambda}{2\chi^2_{r_{max}}}$.

Now let us analyze the relationship between initial conditions and controller gains.

Let us take the simple case that $\mathcal{S}$ is given by: $\mathcal{S} = \{(P_e, \chi_e)/V(P_e, \chi_e) < 2\lambda^3\}$, (we assume that $2\lambda^3 < \frac{k\lambda}{2\chi^2_{r_{max}}}$)

In this case, the domain $\mathcal{S}$ must be bounded by $\theta_e = \pm\pi$. This leads us to find the relationship between the initial configuration error $(P_0^T, \chi_0) = (x_0, y_0, \theta_0, \chi_0)^T$ and the controller gains. Let:

$$V_0 = \frac{\lambda}{2}[kz_0^2 + \lambda^2\mu\chi_0^2 + 4\lambda^2\sin^2(\frac{\theta_0}{2})] < 2\lambda^3 \qquad (29)$$

Since $V(P_e, \chi_e)$ is decreasing in $\mathcal{S}$, it follows:

$$\frac{\lambda}{2}[kz_e^2 + \lambda^2\mu\chi_e^2 + 4\lambda^2\sin^2(\frac{\theta_e}{2})] < 2\lambda^3 \qquad (30)$$

In order to assert that $\theta_e^{max}$ is smaller than $\pi$ the inequality (31) must be satisfied ($v_c$ is assumed to be greater than zero):

$$\lambda^2[2(1+\cos\theta_0 - k\theta_0^2 - \mu\chi_0^2] - 2k\theta_0(y_0+\mu\chi_0)\lambda - k(y_0+\mu\chi_0)^2 > 0 \qquad (31)$$

For example if we consider that ($\chi_0 = 0$) and $2(1+\cos\theta_0) - k\theta_0^2 > 0$, the inequality (31) is satisfied if we take a $\lambda$ greater than $k\theta_0 y_0 + |y_0|\cos\frac{\theta_0}{2}\sqrt{2k}/[2(1+\cos\theta_0) - k\theta_0^2]$.

Finally, for a given domain of possible initial conditions, we can always choose $\lambda$, $k$ and $\mu$ such that the inequality be verified on the domain.

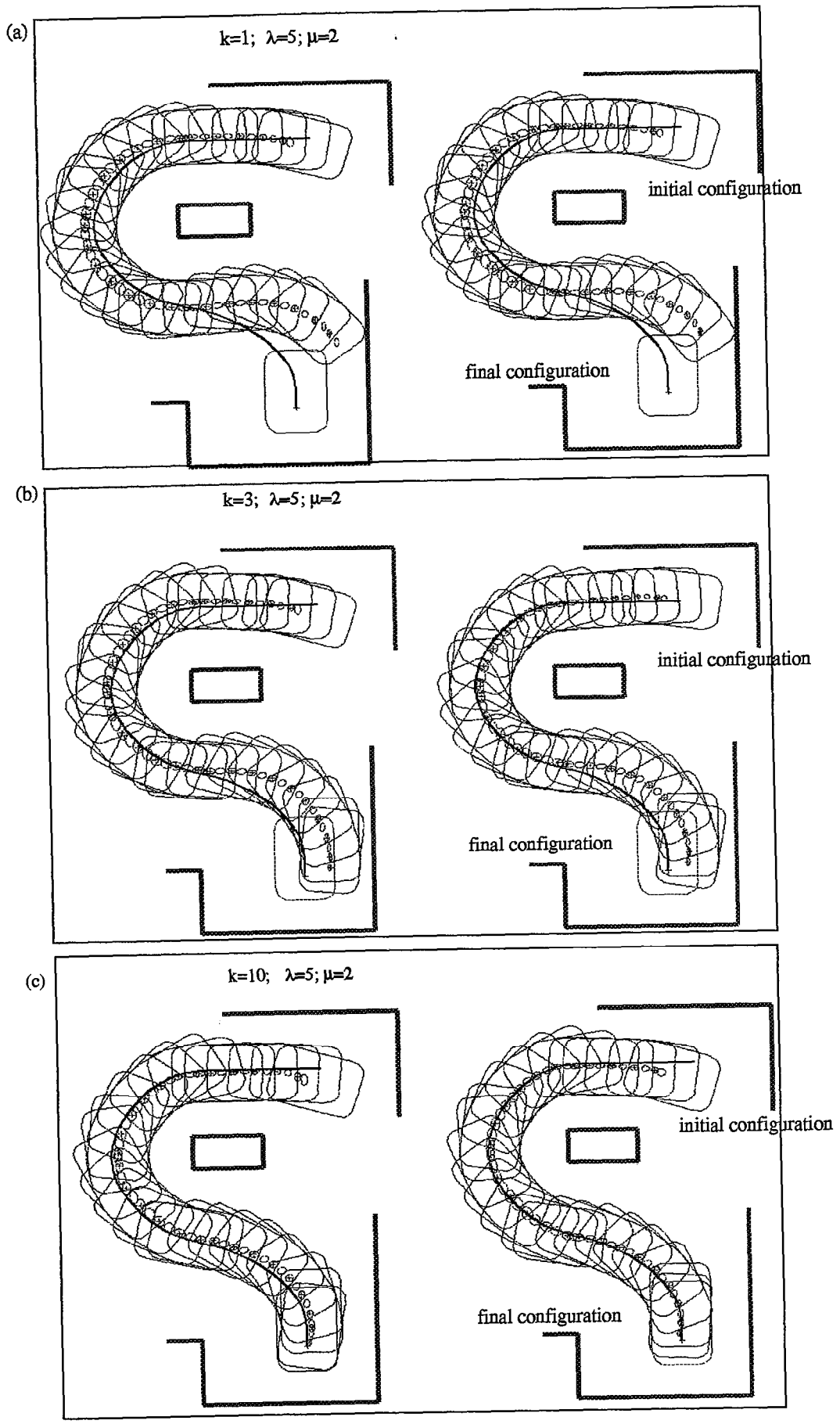


Figure 10: "Experimental results" The realized path for the ROBUTER$^{TM}$